

Francisco J. L. Gordillo · Félix L. Figueroa
F. Xavier Niell

Photon- and carbon-use efficiency in *Ulva rigida* at different CO₂ and N levels

Received: 18 February 2003 / Accepted: 6 July 2003 / Published online: 21 August 2003
© Springer-Verlag 2003

Abstract The seaweed *Ulva rigida* C. Agardh (Chlorophyta) was cultured under two CO₂ conditions supplied through the air bubbling system: non-manipulated air and 1% CO₂-enriched aeration. These were also combined with N sufficiency and N limitation, using nitrate as the only N source. High CO₂ in *U. rigida* led to higher growth rates without increasing the C fixed through photosynthesis under N sufficiency. Quantum yields for charge separation at photosystem II (PSII) reaction centres (ϕ_{PSII}) and for oxygen evolution (ϕ_{O_2}) decreased at high CO₂ even in N-sufficient thalli. Cyclic electron flow around PSII as part of a photoprotection strategy accompanied by decreased antennae size was suspected. The new re-arrangement of the photosynthetic energy at high CO₂ included reduced investment in processes other than C fixation, as well as in carbon diverted to respiration. As a result, quantum yield for new biomass-C production (ϕ^{growth}) increased. The calculation of the individual quantum yields for the different processes involved allowed the completion of the energy flow scheme through the cell from incident light to biomass production for each of the CO₂ and N-supply conditions studied.

Keywords *Ulva* · Absorbance · Chlorophyll fluorescence · Inorganic carbon · Nitrogen limitation · Quantum yield

Abbreviations *A*: total thallus absorbance · *A*_{pig}: absorbance due to pigments · *A*_{str}: Absorbance due to non-pigmented structures · *a*^{*}: spectrally averaged in vivo absorption cross-section of chlorophyll *a* · *CCM*: carbon-concentrating mechanism · *Chl*: chlorophyll · *DOC*: dissolved organic carbon · *ETR*: electron

transport rate · *F_v/F_m*: optimum quantum yield for PSII charge separation · *GP*: gross O₂ evolution rate · *k*_{pig}: specific light absorption coefficient for pigments · *k*_{str}: specific light absorption coefficient for non-pigmented structures · *OP*: optimum O₂ evolution rate · *PFR*: photon fluence rate · *POC*: particulate organic carbon · *PS*: photosystem · *q_N*: non-photochemical quenching · *q_P*: photochemical quenching · ϕ^{growth} : quantum yield for new biomass-C production · ϕ_{O_2} : quantum yield for gross O₂ evolution · ϕ_{PSII} : quantum yield for PSII charge separation

Introduction

One of the main queries for depicting future scenarios for ecosystems is whether the expected increase in atmospheric CO₂ will stimulate primary production. In aquatic environments, to answer this question it is necessary to know not only whether photosynthesis is saturated at the present carbon concentration in the oceans, since many aquatic primary producers possess carbon-concentrating mechanisms (CCMs), but also whether there is a corresponding effect on growth (Riebesell et al. 1993). Thus, the majority of the studies on the effects of increasing CO₂ in aquatic photosynthetic organisms have mainly focused on the uptake of carbon through CCMs, while little attention has been paid to other processes. This has led to a lag in knowledge of the interaction between high CO₂, light-harvesting efficiency and nutrient assimilation in aquatic plants with respect to their terrestrial counterparts.

For terrestrial plants, it has been proposed that the response to elevated CO₂ would be similar to that of nitrogen limitation (Webber et al. 1994). The hypothesis was developed and tested that elevated CO₂ increases photochemical energy use when there is a high demand for assimilates and decreases usage when demand is low. The acceleration of C assimilation through photosynthesis provokes a higher demand for N. If N availability or assimilation rates cannot meet the new demand, a

F. J. L. Gordillo (✉) · F. L. Figueroa · F. X. Niell
Departamento de Ecología, Facultad de Ciencias,
Universidad de Málaga, Campus de Teatinos,
29071 Málaga, Spain
E-mail: gordillo@uma.es
Fax: +34-952-132000

situation equivalent to N limitation develops, and then adaptation mechanisms often resemble those occurring in N limitation under normal CO₂ conditions. This correspondence is not always applicable due to complex interactions between the metabolisms of carbon and nitrogen (e.g. Kruse et al. 2003).

Changes in carbon assimilation at elevated CO₂ necessitate changes in the partitioning of absorbed energy between heat dissipation and photochemistry in the thylakoid membrane (Drake et al. 1997) and in the way photochemical energy is used by the metabolism. Previous studies on the effects of elevated CO₂ on energy partitioning in the photosynthetic apparatus have produced consistent results. Biochemically based models of C-3 photosynthesis can be used to predict that when photosynthesis is limited by the amount of Rubisco, increasing atmospheric CO₂ will increase light-saturated linear electron flow through photosystem II (PSII). This is because the stimulation of electron flow to the photosynthetic carbon reduction cycle will be greater than the competitive suppression of electron flow to the photorespiratory carbon oxidation cycle. Then the ratio of absorbed energy dissipated photochemically to that dissipated non-photochemically will rise (Hymus et al. 2001). In algae possessing CCMs, photorespiration is normally lacking due to high CO₂ concentration around Rubisco even at ambient CO₂ levels in the medium (Beer et al. 2000), so that the model proposed for higher plants is not likely to work in algae with CCMs. Information on how CO₂ will alter energy partitioning between the processes involved in its photochemical conversion to new biomass is very scarce for algae, and particularly so for macroalgae. It has been previously proposed that CO₂ would somehow affect pigment synthesis (García-Sánchez et al. 1994) and photosynthetic apparatus organization (Polle et al. 2000). It seems that CO₂ is involved in the transcription of genes of the light-harvesting complex (LHC; Somanchi et al. 1998) but the functional meaning of such regulation is unknown. Differences in energy partitioning between photosystems at high or low CO₂ has also been reported (Satoh 2002). Higher PSI/PSII reaction-centre ratios under low-CO₂ conditions are thought to reflect the requirement of PSI cyclic electron flow to drive the energy-expensive carbon pump (reviewed by Kaplan and Reinhold 1999).

The flat green macroalga *Ulva* has often been used as a model organism. In *U. rigida* growth is entirely governed by N assimilation, while photosynthesis is CO₂-saturated at current atmospheric levels of CO₂ (Björk et al. 1993; Mercado et al. 1998). In our previous work we reported that growth rate increases at high CO₂ due to photosynthesis-independent stimulation of N assimilation. The corresponding demand for extra C is covered by: (i) reducing losses of organic C being released to the external medium, and (ii) less assimilated C being spent in respiration (Gordillo et al. 2001). How photon capture and energy partitioning can meet these adaptation mechanisms has not been tackled until now.

In this study, we attempt to quantify the quantum yields of the main constraining processes involved in the conversion of photons into biomass production under different CO₂ and NO₃⁻ availability situations. Quantum yield quantifies the efficiency of a light-dependent process and can be determined for individual steps in the photosynthetic chain of events leading to the formation of new biomass. As a result, a complete flow-scheme of energy partition in the cell is presented. We intend to show that CO₂ enrichment can modify not only the photosynthetic performance but also the light-capture strategy and the energy partitioning finally determining the growth efficiency. Mechanisms of adaptation to different CO₂ and NO₃⁻ supply conditions are discussed. Knowing the performance of these processes is an urgent task since excessive growth of *U. rigida* in polluted coastal areas often provokes severe environmental problems (Sfriso 1995).

Materials and methods

Plant cultivation

Ulva rigida C. Agardh was collected in an intertidal rocky shore in Málaga (Mediterranean Sea, Southern Spain). Healthy thalli free from macroscopic epibionts were selected and kept for 3–4 days in filtered (Whatman GF/F) and enriched sea water (Provasoli 1968) at 25 °C, bubbled with air at 1 l min⁻¹, a photoperiod of 12 h:12 h (light:darkness) and a photon fluence rate (PFR) of 100 μmol m⁻² s⁻¹ provided by white fluorescent lamps (Osram daylight L 20 W/10 S). Light in the photosynthetically active range (PAR) range was measured with a spherical sensor (LiCor 193 SB) connected to a LiCor-1000 DataLogger radiometer. The indicated subsaturating PFR was selected to avoid disagreement between measurements of pulse amplitude modulated (PAM) fluorometry and measurements of O₂ evolution rates as observed at saturating PFRs in *Ulva*, according to Beer et al. (2000), Frankling and Badger (2001), and Longstaff et al. (2002).

Experimental design

Cultures ran for 10 days under two CO₂ conditions: non-manipulated air (current atmospheric concentration: 0.035%) and CO₂-enriched aeration (1%); combined with two initial N concentrations added in batch mode: N sufficiency (5 mM NO₃⁻) and N limitation (0.25 mM NO₃⁻, net uptake ceased after 4 days). The CO₂ enrichment would correspond to 360 μM CO₂, 22.51 mM HCO₃⁻, and 1.13 mM CO₃⁻ dissolved in the culture medium at equilibrium.

Thalli were cut into discs of 2 cm in diameter for cultivation. Cultures started when 1.5 g FW were placed in an Erlenmeyer flask containing 1 l filtered seawater (Millipore 0.22 μm) enriched with Provasoli-based medium (Provasoli 1968). Temperature, aeration, PFR and photoperiod were the same as for maintenance conditions described above. The water motion produced by the aeration allowed the discs to move softly without tumbling.

The pH in CO₂-enriched cultures was never below 7.7. A control culture at pH 7.7 without CO₂ enrichment eliminated any statistically significant influence of pH on the results.

Light absorption

Chlorophyll (Chl) *a*, Chl *b* and total carotenoids were extracted from fresh discs in N,N-dimethyl formamide for 24 h at room temperature and total darkness. The concentrations were determined spectrophotometrically according to Wellburn (1994).

Total thallus absorbance for the PAR region (A) was estimated spectrophotometrically by the opal-glass method according to Mercado et al. (1996). The fraction of A due to pigments (A_{pig}) and due to structures ($A_{\text{str}} = A - A_{\text{pig}}$) was calculated from the equations given by Markager and Sand-Jensen (1994), except that calculations were based on thallus area instead of thallus-specific carbon content:

$$A = 1 - e^{-(k_{\text{pig}}[\text{pig}] + k_{\text{str}} w/a)} \quad (1)$$

$$A_{\text{pig}}/A = (k_{\text{pig}}[\text{pig}]) / (k_{\text{pig}}[\text{pig}] + k_{\text{str}} w/a) \quad (2)$$

where k_{pig} is the specific light-absorption coefficient for pigments ($\text{m}^2 \text{g}^{-1}$ total pigments), $[\text{pig}]$ is the total pigment concentration (g m^{-2}), k_{str} is the specific light-absorption coefficient for non-pigmented structures of the thallus ($\text{m}^2 \text{g}^{-1}$ DW) and w/a is the ratio dry weight to area (g DW m^{-2}).

Photosynthetic parameters

Net photosynthesis at saturating PFR (P_{max} , $600 \mu\text{mol m}^{-2} \text{s}^{-1}$) and at culture PFR (NPS, $100 \mu\text{mol m}^{-2} \text{s}^{-1}$) and dark respiration rates were estimated by oxygen evolution using a Clark-type oxygen electrode (Yellow Spring Instruments, 5331) in a 9-ml custom-made transparent Plexiglas chambers at 25°C . Rate measurements were made at 10-min intervals. To allow the conversion from evolved O_2 to fixed CO_2 , the photosynthetic quotient (PQ) was estimated by measuring changes in pH, simultaneously to O_2 in the photosynthesis chambers, and converted to CO_2 by the program SEAWATER (David Turner, Plymouth). Optimal quantum yield for PSII fluorescence (F_v/F_m) was measured by means of a pulse amplitude modulated fluorimeter (PAM-2000; Waltz, Effeltrich, Germany) after 15 min of incubation in darkness. Under culture conditions, effective quantum yield of PSII ($\phi_{\text{PSII}} = \Delta F/F_m'$), as well as the photochemical (q_p) and non-photochemical quenching (q_N) were also measured using the same apparatus. According to Genty et al. (1989), F_v is the maximal variable fluorescence of a dark-adapted sample, F_m the fluorescence intensity with all PSII reaction centres closed, F the fluorescence at any time during induction and F_m' the light-saturated fluorescence. The electron transport rate between PSII and PSI (ETR) was calculated as:

$$\text{ETR} = \Phi_{\text{PSII}} \cdot \text{PFR} \cdot 0.5 \cdot A_{\text{pig}}$$

where 0.5 stands for the assumption of equal contribution of excitons between PSI and PSII.

For clarity in the discussion of processes, we preferred to use the PSII excitation pressure ($1 - q_p$), rather than q_p . Thus, $1 - q_p$ would indicate the proportion of reduced Q_A , the primary PSII acceptor. All measurements were performed after 10 days of cultivation.

Total internal C and particulate organic carbon (POC)

Total internal organic C was measured with a C:H:N elemental analyser (Perkin-Elmer 2400CHN) after drying three discs from each culture overnight at 80°C . For POC in the culture medium, water samples from the culture medium were filtered (Whatman GF/F). The filter was dried overnight at 80°C and used for determination of POC using the C:H:N elemental analyser.

Determination of dissolved organic carbon (DOC)

Daily water samples for the determination of DOC in the medium were analysed in an automated system (Traacs 800; Bran & Luebbe) by means of the persulfate oxidation method which includes UV radiation, CO_2 dialysis and colorimetric determination (Koprivnjak et al. 1995).

Statistics

Data presented are the mean of three independent experiments, each consisting of two cultures running in parallel for each treatment. Results were compared by two-way analyses of variance followed by a multirange test using Fisher's protected least significant differences (LSD). The confidence level was set at 5%.

Results

Cell contents of Chl a , Chl b and total carotenoids decreased at high CO_2 , especially Chl b which lost 25% with respect to normal CO_2 levels in N sufficiency (Table 1). As a consequence, the ratio Chl b/a showed lower values at high CO_2 . Nitrogen limitation also reduced the pigment content; this inhibitory effect was in addition to that promoted by high CO_2 , so that thalli grown at high CO_2 and N limitation showed the poorest pigmentation. However, this additive effect did not significantly affect the ratio Chl b/a . Changes in the spectrally averaged in vivo absorption cross-section of Chl a (a^*) denote changes in the optical properties, structure and composition of the chloroplasts according to Berner et al. (1989). The a^* values resulted in a 50% increase at high CO_2 in N sufficiency reaching $9 \text{ m}^2 \text{g}^{-1}$ Chl a . This increase was lower in N-limiting conditions.

Total pigment content was plotted against total thallus absorbance for the PAR region (A , Fig. 1) in order to differentiate between the absorption due to pigments (A_{pig}) and that due to non-pigmented structures (A_{str}). Data in Fig. 1 were fitted to the equation given by Markager and Sand-Jensen (1994), described above (Eq. 1; $r = 0.88$, $P < 0.05$), from which:

$$k_{\text{pig}} = 2.68 \text{ m}^{-2} \text{g}^{-1} \text{ total pigments}$$

$$k_{\text{str}} = 0.014 \text{ m}^{-2} \text{g}^{-1} \text{ DW}$$

Table 2 shows the values of thallus total absorbance (A) for the different treatments, as well as its two components, A_{pig} and A_{str} . In N sufficiency, A values were slightly higher at high CO_2 , due to an increase in A_{str} rather than A_{pig} which remained unchanged at 0.45; i.e., 45% of the incident light was absorbed by pigments

Table 1 Pigment composition (mg g^{-1} DW) and ratio, and a^* values ($\text{m}^2 \text{g}^{-1}$ Chl a) of *Ulva rigida* cultured with non-enriched (Air) and 1% CO_2 -enriched air (+ CO_2), in N-sufficient (N+), and N-limited (N-) conditions. Standard deviations in parentheses ($n = 6$); different superscripts indicate significant differences ($P < 0.05$)

Parameter	Air		+ CO_2	
	N+	N-	N+	N-
Chl a	6.9 (0.7) ^a	4.3 (0.4) ^b	5.6 (0.5) ^c	2.5 (0.6) ^d
Chl b	5.6 (0.5) ^a	3.1 (0.3) ^b	4.2 (0.3) ^c	1.7 (0.5) ^d
Total	2.8 (0.3) ^a	1.6 (0.2) ^b	2.3 (0.2) ^c	1.0 (0.2) ^d
carotenoids				
Chl b/a	0.82 (0.03) ^a	0.73 (0.02) ^b	0.74 (0.02) ^b	0.70 (0.03) ^b
a^*	6.2 (0.6) ^a	5.9 (1.1) ^a	9.0 (1.4) ^b	7.6 (2.5) ^{ab}

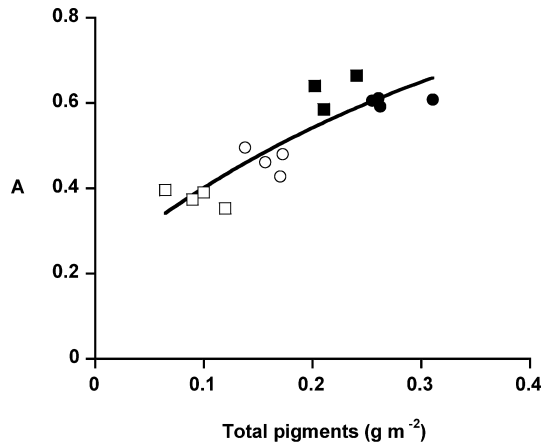


Fig. 1 Relationship between total thallus absorbance (A) and pigment concentration in *Ulva rigida*. Curve fitting ($r=0.88$, $P<0.05$) corresponds to the equation given by Markager and Sand-Jensen (see Eq. 1 in the text). *Closed circles* N-sufficient samples with non-manipulated air, *open circles* N-limited samples with non-manipulated air, *closed squares* N-sufficient samples with 1% CO_2 -enriched air, *open squares* N-limited samples with 1% CO_2 -enriched air

Table 2 Quantum yields of processes involved in light absorption. Total (A) and pigmentary (A_{pig}) and non-pigmentary absorbances ($A_{\text{str}} = A - A_{\text{pig}}$), as well as optimal (F_v/F_m) and effective (ϕ_{PSII}) PSII quantum yield of *U. rigida* cultured with non-enriched (Air) and 1% CO_2 -enriched air (+ CO_2), in N-sufficient (N+), and N-limited (N-) conditions. Standard deviations in parentheses ($n=6$); different superscripts indicate significant differences ($P<0.05$)

Parameter	Air		+ CO_2	
	N+	N-	N+	N-
A	0.60 (0.00) ^a	0.52 (0.03) ^b	0.64 (0.02) ^c	0.48 (0.02) ^b
A_{pig}	0.45 (0.01) ^a	0.36 (0.01) ^b	0.45 (0.02) ^a	0.29 (0.02) ^c
A_{str}	0.15 (0.01) ^a	0.16 (0.01) ^a	0.19 (0.01) ^b	0.19 (0.01) ^b
F_v/F_m	0.70 (0.00) ^a	0.62 (0.03) ^b	0.73 (0.01) ^a	0.55 (0.05) ^c
ϕ_{PSII}^*	0.53 (0.00) ^a	0.38 (0.02) ^b	0.40 (0.01) ^b	0.18 (0.02) ^c

*Measured at $\text{PFR} = 100 \mu\text{mol m}^{-2} \text{s}^{-1}$

in N sufficiency, regardless the CO_2 treatment. However, the impact of N limitation on A_{pig} was more noticeable at high CO_2 where values dropped to 0.29. The optimum and effective quantum yield for charge separation at PSII reaction centres (F_v/F_m and ϕ_{PSII} , respectively) are also shown in Table 2. F_v/F_m remained unchanged at high CO_2 in N sufficiency, but not so ϕ_{PSII} , which significantly decreased from 0.53 to 0.40 at culture PFR. As for A_{pig} , the influence of N limitation on decreasing both F_v/F_m and ϕ_{PSII} was greater at high CO_2 .

Linear electron transport rates between photosystems (ETR) are represented in Fig. 2a. The initial slope of the curve, named the photosynthetic efficiency (α), was affected by CO_2 enrichment only under N limitation; however, the maximum ETR (ETR_{max}) decreased both due to CO_2 enrichment and N limitation, so that the lowest ETR was found at high CO_2 under N limitation. Nitrogen limitation did not promote significant differences in PSII excitation pressure ($1-q_p$), at least at PFR

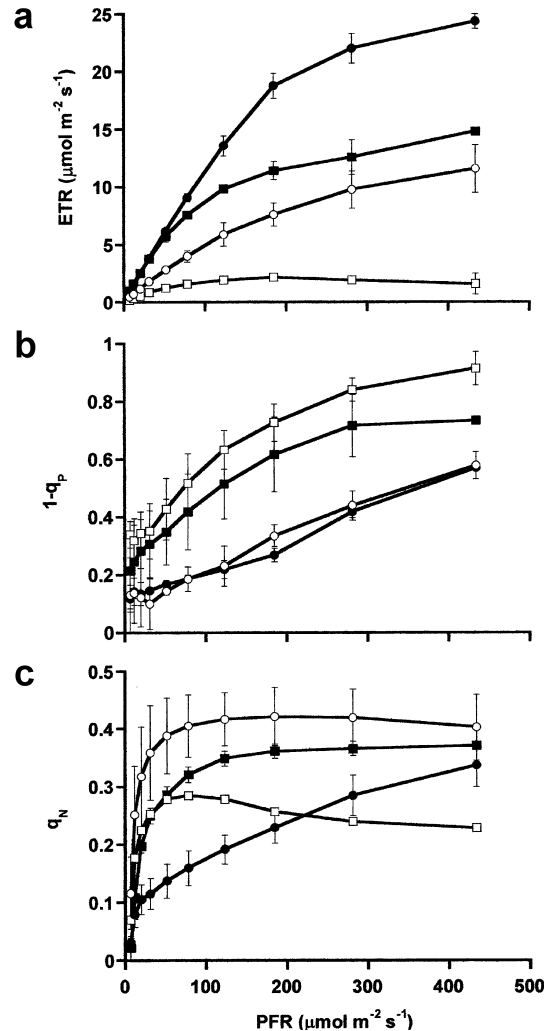


Fig. 2a–c Electron transport rates (a), PSII excitation pressure (b), and non-photochemical quenching (c) at increasing PFR of *U. rigida* cultured at different CO_2 and N-supply conditions. *Closed circles* N-sufficient samples with non-manipulated air, *open circles* N-limited samples with non-manipulated air, *closed squares* N-sufficient samples with 1% CO_2 -enriched air, *open squares* N-limited samples with 1% CO_2 -enriched air

below $300 \mu\text{mol m}^{-2} \text{s}^{-1}$ (Fig. 2b). Increased CO_2 led to higher excitation pressure regardless of the N conditions to near saturation beyond $300 \mu\text{mol m}^{-2} \text{s}^{-1}$. Both N limitation and increased CO_2 led to an early saturation of energy dissipation measured as q_N (Fig. 2c) with respect to the control conditions as PFR increased. Final q_N values at saturating irradiance were similar for all culture conditions except for high CO_2 + N limitation.

The fate of the carbon fixed through photosynthesis is represented as a percentage relative to the control culture (air, N+) in Table 3. The level of CO_2 conditioned both the total value and the relative proportion of the different processes involved. At low CO_2 the impact of N limitation was only 5%, while at high CO_2 the reduction respect to N sufficiency was almost 20%. The percentage of C diverted to respiration was markedly reduced at high CO_2 under both N conditions. At high

Table 3 Comparative carbon use by *U. rigida* under different CO₂ and N supply situations expressed as a percentage of the total carbon fixed by the control culture (air, N+). Samples were cultured for 10 days with non-enriched (Air) and 1% CO₂-enriched air (+CO₂), in N-sufficient (N+) and N-limited (N-) conditions. Standard deviations in parentheses (*n*=6); different superscripts indicate significant differences (*P*<0.05)

	Air		+CO ₂	
	N+	N-	N+	N-
Respiration	73.84 (2.67) ^a	75.62 (2.66) ^a	34.7 (1.78) ^b	40.92 (0.89) ^c
POC	4.54 (0.15) ^a	5.07 (0.16) ^b	4.8 (0.29) ^a	4.63 (0.12) ^a
DOC	2.94 (0.1) ^a	4.09 (0.13) ^b	2.76 (0.17) ^a	5.6 (0.13) ^c
Growth	18.68 (2.34) ^a	10.68 (3.56) ^b	39.15 (3.01) ^c	11.56 (4.45) ^b
Total	100	95.46	81.4	62.72

Table 4 Quantum yields for oxygen evolution based on light absorbed by pigment (ϕ_{O_2} =mol O₂:mol photons); and quantum yields for net growth (ϕ_{i}^{growth} =mol C:mol photons) based on incident light (*i*), total absorbed light (*A*) and light absorbed by pigments (*pig*) in *U. rigida*. Samples were cultured for 10 days with non-enriched (Air) and 1% CO₂-enriched air (+CO₂), in N-sufficient (N+), and N-limited (N-) conditions. Standard deviations in parentheses (*n*=6); different superscripts indicate significant differences (*P*<0.05)

	Air		+CO ₂	
	N+	N-	N+	N-
ϕ_{O_2}	0.118	0.106	0.086	0.197
Φ_i^{growth}	0.021 (0.006) ^a	0.012 (0.004) ^a	0.044 (0.009) ^b	0.013 (0.005) ^a
Φ_A^{growth}	0.034 (0.009) ^a	0.023 (0.008) ^a	0.069 (0.014) ^b	0.027 (0.010) ^a
Φ_{pig}^{growth}	0.045 (0.012) ^a	0.034 (0.012) ^a	0.098 (0.022) ^b	0.044 (0.017) ^a

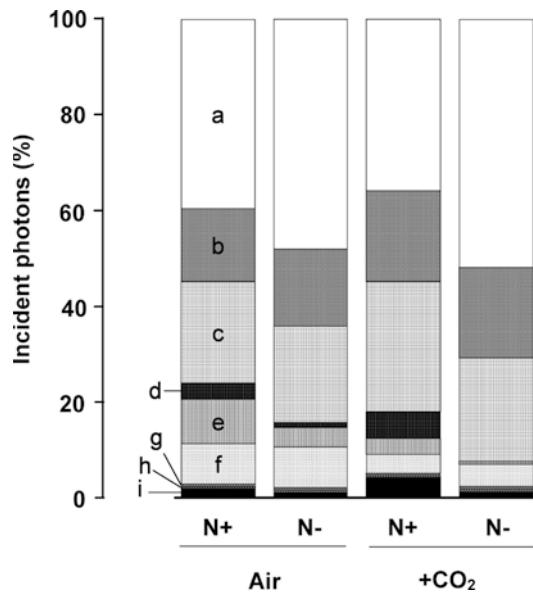


Fig. 3 Energy distribution of incident light among different processes as it flows from the thallus surface (top) to the production of new biomass-C (bottom), expressed as a percentage. *a* Transmitted through; *b* absorbed by non-pigmented structures; *c* dissipated in the photosynthetic antennae; *d* suboptimal O₂ production, assuming the optimal to be eight electrons per gross O₂ evolved; *e* photosynthetic energy available for processes other than C fixation; *f* fixed carbon lost by respiration; *g*, *h* organic carbon released and found in the medium in particulate and dissolved form, respectively; *i* fixed carbon invested in new biomass production

CO₂ in N sufficiency, the percentage invested in growth was the highest, despite total C fixed being lower than the control. N limitation led to the lowest investment of C into new biomass regardless of the CO₂ conditions.

The energy flow through the cell can be quantified and represented as in Fig. 3. The total height of the column represents the total amount of photons by units of area exposed (1/2 of total thallus area) that reached the thallus during the culture period. This energy suffered different losses before getting to form new biomass carbon. The first loss of energy, neglecting

reflectance, is that not being absorbed by the thallus and then transmitted through [a, (1-A)×100]. This was higher in N limitation. Part of the energy was absorbed by non-pigmented structures [b, (A-A_{pig})×100], the rest being absorbed by pigments. Light absorbed by pigments decreased by N limitation but was not affected by CO₂. Of that energy, part was dissipated as a radiationless decay from the antennae in their way to the reaction centres [c, [(1- ϕ_{PSII}) A_{pig}]×100]. This loss was slightly higher at high CO₂. The box d represents suboptimal conversion of excitons to oxygen evolved, assuming an optimal conversion of eight electrons per O₂ (i.e. ϕ_{O_2} =0.125 O₂ per photon), according to the Z-scheme for photosynthesis {[1-(GP/OP) ϕ_{PSII} A_{pig}]×100}, where GP is gross photosynthesis (i.e. measured gross O₂ evolution rate) and OP the optimum photosynthesis (i.e. maximum O₂ that should have been produced if operating at eight electrons per O₂). Then, this represents the disagreement between the observed O₂ evolution in the photosynthetic chambers and that calculated according to the number of photons estimated to reach the reaction centres divided by eight. Under normal (non-enriched) CO₂ conditions the electron demand per oxygen evolved was close to the optimum, with values of 8.5 and 9.3 for N-sufficient and N-limited thalli, respectively (i.e. ϕ_{O_2} of 0.118 and 0.106, respectively; Table 4). CO₂ enrichment altered this step in different ways depending on N conditions. Under N sufficiency more than 11 electrons were needed per O₂ evolved, whereas under N limitation a controversial value of 5 was estimated. The box e in Fig. 3 represents the amount of photosynthetic energy remaining after carbon fixation. This remaining photosynthetic energy would be available for other processes such as CCMs, nutrient uptake and biosynthesis of macromolecules. In Fig. 3, box e is calculated then as {[(GP/OP) ϕ_{PSII} A_{pig}]×100 - (f+g+h+i)}. This portion of energy decreased both with CO₂ enrichment and with N limitation. Box f represents the portion of photosynthetic energy invested in fixing C that was lost in the respiration process [(Dark resp./OP) ϕ_{PSII} A_{pig} × 100]. Respiration markedly

decreased at high CO₂, especially under N sufficiency. Box g is the portion corresponding to fixed carbon released to the external medium and found in particulate form [(POC/OP) $\phi_{\text{PSII}} A_{\text{pig}} \times 100$]; box h is the percentage corresponding to fixed carbon released to the external medium and found in dissolved form [(DOC/OP) $\phi_{\text{PSII}} A_{\text{pig}} \times 100$]. Finally, box i represents the percentage of incident energy that was invested in fixing carbon to form new biomass, i.e. net growth [(total internal carbon in the new biomass/OP) $\phi_{\text{PSII}} A_{\text{pig}} \times 100$). This portion decreased under N-limiting conditions for both CO₂ situations but it increased at high CO₂ when N was supplied in excess.

Table 4 shows the quantum yields for net growth based on incident light (Φ_i^{growth}), total absorbed light (Φ_A^{growth}) and light absorbed by pigments ($\Phi_{\text{pig}}^{\text{growth}}$). Results indicate that provided N is not limiting, the efficiency in the use of light is practically double at high CO₂ with respect to non-manipulated-air conditions. When quantum yield is expressed in terms of light absorbed by pigments, growth efficiency got to 0.098, close to the theoretical maximum of 0.125.

Discussion

The portion of incident light absorbed by non-pigmented structures (A_{str}) was quite significant for all treatments. This enforces the suggestion that this factor should be taken into account in order to determine the proportion of incident light that is actually absorbed by the antennae pigments (A_{pig}). Uncertainties on such estimations would lead to a limited knowledge of ETR as measured by pulse amplitude modulated fluorometry, as previously discussed by Beer et al. 2000 and Frankling and Badger 2001; however, very few studies on ETR include this sort of measurement. This is due, at least in part, to the difficulty of performing good estimates in species with thick thallus structure. Another assumption remains: we have ignored the portion of light being back-scattered, although this is likely to be less than 1% under a perpendicular light beam (Frost-Christensen and Sand-Jensen 1992). The values of A measured agreed with those reported by Frankling and Badger (2001) for *U. australis*, and A_{str} was close to the value given by Markager and San-Jensen (1994) of 0.13 for *U. lactuca*.

Changes in pigment composition triggered by increased CO₂ are a frequently observed response. García-Sánchez et al. (1994) and Nakano et al. (1997) reported a significant decrease in Chl *a* concentration in the red macroalga *Gracilaria tenuistipitata* and in rice leaves, respectively, in a CO₂-enriched environment; other plants, such as the seagrass *Zostera marina* (Zimmerman et al. 1997), the green microalga *Scenedesmus obtusiusculus* (Larsson et al. 1985) and the brown alga *Fucus serratus* (Johnston and Raven 1990) did not show any change in their pigment concentration. A hypothesis has been previously suggested according to which the

decrease in pigment content at high CO₂ would correspond to the elimination of molecules that are in excess and would not participate efficiently in the light capture for photosynthesis, after a new rearrangement of the light-harvesting system as part of the acclimation strategy. This has been called “the pigment economy hypothesis” (Gordillo et al. 1999). This is supported by the fact that the optimal quantum yield for charge separation at PSII reaction centres (F_v/F_m) and the initial slope of the ETR–PFR curves are the same at high and low CO₂ (in N sufficiency). A complementary hypothesis suggests that lower pigment content at high CO₂ could be an adaptation reducing the antenna size to avoid over-excitation of electron transport, although this might not affect the electron transport chain itself (Saxe et al. 1998). This is in agreement with the decrease in the Chl*b/a* ratio and the increase in a^* observed. Similar results have been found for the unicellular chlorophyte *Dunaliella viridis* (Gordillo et al. 2003) and the cyanobacterium *Spirulina platensis* (Gordillo et al. 1999) under equivalent culture conditions.

Differences in ETR_{max} can be attributed to differences in the amount of Rubisco present in the chloroplast. The fall in final values of the ETR curves when either increasing CO₂ or limiting N coincided with the fall in the pool of soluble proteins reported previously (Gordillo et al. 2001), of which Rubisco constitutes a majority. The increase in excitation pressure ($1-q_p$) observed at high CO₂ (Fig. 2b) indicates the establishment of a mechanism of over-excitation of the quinone pool that was not provoked by an increase in the amount of charge separations at PSII, since ETR was even lower at high CO₂. Cyclic flow around PSII as a photoprotective resource is a possible explanation, as discussed below. The increase in non-photochemical quenching is one of the first responses to environmental stress. In *U. rigida*, both high CO₂ and N limitation increased q_N at intermediate PFRs (Fig. 2c), evidencing an early establishment of energy dissipation processes.

Values of ϕ_{O_2} close to the optimum of 0.125 measured under control CO₂ conditions were in agreement with those found by Beer et al. (2000) for *U. lactuca* and *U. fasciata*. Frankling and Badger (2001) found that closeness to optimal values was CO₂-dependent in *U. australis* and other macroalgae. We found that up to 11 electrons were needed to produce 1 O₂ molecule at high CO₂ in N-sufficient thalli. According to Frankling and Badger (2001), ETR in excess of O₂ evolution in *Ulva* is unlikely to represent higher photorespiration rates or Mehler activity. The alternative explanation given by these authors is cyclic electron flow around PSII from the quinone acceptor Q_B (Pheophytin) via cyt *b*₅₅₉. In the case where electrons cannot be re-supplied to P₆₈₀₊ from the water oxidation complex, the strong oxidant P₆₈₀₊ can be re-reduced by cyt *b*₅₅₉, preventing the oxidation of nearby elements of the reaction centre. This mechanism would provide additional photoprotective capacity for keeping PSII active without O₂ evolution or photosynthetic energy

production. Lavaud et al. (2002) found that up to three extra excitons would be needed at PSII for O₂ evolution, preventing both acceptor-side photoinhibition in oxygen-evolving PSII and donor-side photoinhibition when the oxygen-evolving complex is temporarily inactivated. The 11 electrons needed per O₂ and higher reduction status of the Q_A (1-*q_p*) observed at high CO₂ (Fig. 2b) would support this interpretation. Another reason for a deviation from the optimum at high CO₂ (in N sufficiency) could be the difference in light-capture efficiency by PSI and PSII. CO₂ has been reported to affect light-capture efficiency of PSI to a larger extent than that of PSII (Sato et al. 2002). Bürger et al. (1988) and Miyachi et al. (1996) found in some cyanobacteria and unicellular green algae that both the ratio PSI/PSII and ϕ_{O_2} decreased in cells grown at high CO₂. The higher PSI/PSII under low CO₂ conditions is thought to reflect the demand of the excess energy from PSI for cyclic electron flow to drive the CCMs, as previously suggested by Ogawa and Ogren (1985). When both high CO₂ and N limitation conditions were simultaneously applied, a controversial value of $\phi_{O_2} = 0.2$ was derived. It is known that nitrogen limitation also has differential effects on photosynthetic efficiency of PSI and PSII (Berges et al. 1996). Therefore, since all calculations of ϕ_{O_2} assume equal distribution of photons between PSI and PSII according to the Z-scheme (four photons each), further investigations are needed to elucidate whether this assumption can be made without significant error.

The main difference between higher plants and algae possessing CCMs with respect to elevated CO₂ is the way in which the use of photochemical energy is altered. In higher plants, elevated CO₂ partial pressure leads to decreased photorespiration rates, and then concomitant increased carboxylation efficiency is observed (e.g. Habash et al. 1995). However, many algae, among them *Ulva*, have virtually no photorespiration at current CO₂ levels (Beer et al. 2000) due to the existence of energetically expensive CCMs which increase the level of CO₂ around Rubisco. When exposed to CO₂-enriched conditions, the expression and activity of CCMs are generally repressed (Björk et al. 1993; Gordillo et al. 2001) and the energy normally being invested in such concentrating processes is made available to other processes (Raven 1991). That could be the case for N-sufficient *U. rigida*. Both the portion of photosynthetic energy available for processes other than carboxylation (box e in Fig. 3) and the energy from respiration (box f in Fig. 3) decreased markedly. That being the case, photosynthetic CO₂ fixation does not necessarily increase at high CO₂, whilst cell growth (box i in Fig. 3) reaches higher efficiency (i.e. higher ϕ^{growth}). A question remains whether CCMs at control CO₂ conditions would use energy from photosynthesis or from respiration. Huertas et al. (2002) have recently demonstrated that the source of energy for active CO₂ transport across the membrane comes from photosynthetic electron transport in the unicellular chlorophyte *Nannochloris*

atomus, a species that, unlike *U. rigida* (Björk et al. 1992), lacks an active HCO₃⁻ transporter and extracellular carbonic anhydrase.

At high CO₂, the photosynthetic energy not invested in C fixation or CCMs could well serve for nitrate assimilation. *U. rigida* is a nitrophilic organism and growth stimulation at high CO₂ is known to be governed by an increase in N assimilation (Gordillo et al. 2001), i.e. a higher portion of energy has to be invested in nitrate transport and reduction. In the C4 sorghum, Watling et al. (2000) found that the ratio ϕ_{CO_2} to ϕ_{PSII} was lower in plants grown at elevated CO₂, implying increased electron transport to acceptors other than CO₂.

In conclusion, elevated CO₂ changed the energy capture and partitioning characteristics of *U. rigida*, such that acclimation to high CO₂ implied a different pattern of energy flow through the cell mainly characterised by decreased energy demands for CCMs and lower respiration rates, leading to a more efficient use of photons for growth, despite lower ϕ_{O_2} . The latter was possibly a consequence of photoprotection of PSII reaction centres by suspected cyclic flow around PSII accompanied by decreased antenna size.

Acknowledgements This work was financed by the Spanish Ministry of Science and Technology Project REN 2002-00340/MAR, and the Andalusian research group RNM0176.

References

- Beer S, Larsson C, Poryan O, Axelsson L (2000) Photosynthetic rates of *Ulva* (Chlorophyta) measured by pulse amplitude modulated (PAM) fluorometry. *Eur J Phycol* 35:69–74
- Berges JA, Charlebois DO, Mauzerall DC, Falkowski PG (1996) Differential effects of nitrogen limitation on photosynthetic efficiency of photosystems I and II in microalgae. *Plant Physiol* 110:689–696
- Berner T, Dubinsky Z, Wyman K, Falkowski, PG (1989) Photoadaptation and the “package” effect in *Dunaliella tertiolecta* (Chlorophyceae). *J Phycol* 25:70–78
- Björk M, Haglund K, Ramazanov Z, García-Reina G, Pedersen M (1992) Inorganic-carbon assimilation in the green seaweed *Ulva rigida* C. Ag. (Chlorophyta). *Planta* 187:152–156
- Björk M, Haglund K, Ramazanov Z, Pedersen M (1993) Inducible mechanisms for HCO₃⁻ utilisation and repression of photorespiration in protoplasts and thalli of three species of *Ulva* (Chlorophyta). *J Phycol* 29:166–173
- Bürger J, Miyachi S, Galland P, Senger H (1988) Quantum requirements of photosynthetic oxygen evolution and 77 K fluorescence emission spectra in unicellular green algae grown under low- and high-CO₂ conditions. *Bot Acta* 101:229–232
- Drake B, González-Meler M, Long SP (1997) More efficient plants: a consequence of rising atmospheric CO₂. *Annu Rev Plant Physiol Plant Mol Biol* 48:609–639
- Frankling LA, Badger MR (2001) A comparison of photosynthetic electron transport rates in macroalgae measured by pulse amplitude modulated chlorophyll fluorometry and mass spectrometry. *J Phycol* 37:756–767
- Frost-Christensen H, Sand-Jensen K (1992) The quantum efficiency of photosynthesis in macroalgae and submersed angiosperms. *Oecologia* 91:377–384
- García-Sánchez MJ, Fernández JA, Niell FX (1994) Effects of inorganic carbon supply on the photosynthetic physiology of *Gracilaria tenuistipitata*. *Planta* 194:55–61

- Genty B, Brintais JM, Baker NR (1989) The relationship between the quantum yield of photosynthetic electron transport and quenching of chlorophyll fluorescence. *Biochim Biophys Acta* 990:87–92
- Gordillo FJL, Jiménez C, Figueroa FL, Niell FX (1999) Effects of increased atmospheric CO₂ and N supply on photosynthesis, growth and cell composition of the cyanobacterium *Spirulina platensis* (*Arthrospira*). *J Appl Phycol* 10:461–469
- Gordillo FJL, Niell FX, Figueroa FL (2001) Non-photosynthetic enhancement of growth by high CO₂ level in the nitrophilic seaweed *Ulva rigida* C. Agardh (Chlorophyta). *Planta* 213:64–70
- Gordillo FJL, Jiménez C, Figueroa FL, Niell FX (2003) Influence of elevated CO₂ and nitrogen supply on the carbon assimilation performance and cell composition of the unicellular alga *Dunaliella viridis*. *Physiol Plant* (in press)
- Habash DZ, Paul MJ, Parry MAJ, Keys AJ, Lawlor DW (1995) Increased capacity for photosynthesis in wheat grown at elevated CO₂: the relationship between electron transport and carbon metabolism. *Planta* 197: 482–489
- Huertas IE, Espie GS, Colman B (2002) The energy source for CO₂ transport in the marine microalga *Nannochloris atomus*. *Planta* 214:947–953
- Hymus GJ, Baker NR, Long SP (2001) Growth in elevated CO₂ can both increase and decrease photochemistry and photoinhibition of photosynthesis in a predictable manner. *Dactylois glomerata* grown in two levels of nitrogen nutrition. *Plant Physiol* 127:1205–1211
- Johnston AM, Raven JA (1990) Effects of culture in high CO₂ on the photosynthetic physiology of *Fucus serratus*. *Br Phycol J* 25:75–82
- Kaplan A, Reinhold L (1999) CO₂ concentrating mechanisms in photosynthetic microorganisms. *Annu Rev Plant Physiol Plant Mol Biol* 50:539–570
- Koprivnjak JF, Blanchette JG, Bourbonniere RA, Clair TA, Heyes A, Lum KR, McCrea R, Moore TR (1995) The underestimation of concentrations of dissolved organic-carbon in freshwaters. *Water Res* 29:91–94
- Kruse J, Hetzger I, Mai C, Polle A, Rennenberg H (2003) Elevated pCO₂ affects N-metabolism of young poplar plants (*Populus tremula* × *P. alba*) differently at deficient and sufficient N-supply. *New Phytol* 157:65–81
- Larsson M, Larsson CM, Guerrero MG (1985) Photosynthetic nitrogen metabolism in high and low CO₂-adapted *Scenedesmus*. II. Effect of ammonium and methionine sulphoximine on nitrate utilization. *J Exp Bot* 36:1387–1395
- Lavaud J, van Gorkom HJ, Etienne AL (2002) Photosystem II electron transfer cycle and chlororespiration in planktonic diatoms. *Photosynth Res* 74:51–59
- Longstaff BJ, Kildea T, Runcie JW, Cheshire A, Dennison WC, Hurd C, Kana T, Raven JA, Larkum AWD (2002) An in situ study of photosynthetic oxygen exchange and electron transport rate in the marine macroalga *Ulva lactuca* (Chlorophyta). *Photosynth Res* 74:281–293
- Markager S, Sand-Jensen K (1994) The physiology and ecology of light-growth relationship in macroalgae. In: Round FE, Chapman DJ (eds) *Progress in phycological research*. Biopress, Bristol, pp 209–298
- Mercado JM, Jiménez C, Niell FX, Figueroa FL (1996) Comparison of methods for measuring light absorption by algae and their application to the estimation of the package effect. *Sci Mar* 60:39–45
- Mercado JM, Gordillo FJL, Figueroa FL, Niell FX (1998) External carbonic anhydrase and affinity for inorganic carbon in intertidal macroalgae. *J Exp Mar Biol Ecol* 221:209–220
- Miyachi S, Bürger J, Kotzabasis K, Thielmann J, Senger H (1996) Photosynthetic characteristics of three strains of cyanobacteria grown under low- or high-CO₂ conditions. *Z Naturforsch Teil C* 51:40–46
- Nakano H, Makino A, Mae T (1997) The effect of elevated partial pressure of CO₂ on the relationship between photosynthetic capacity and N content in rice leaves. *Plant Physiol* 115:191–198
- Ogawa T, Ogren WL (1985) Action spectra for accumulation of inorganic carbon in cyanobacterium *Anabaena variabilis*. *Photochem Photobiol* 41:583–587
- Polle JEW, Benemann JR, Tanaka A, Melis A (2000) Photosynthetic apparatus organization and function in the wild type and the chlorophyll *b*-less mutant of *Chlamydomonas reinhardtii*. Dependence on carbon source. *Planta* 211:335–344
- Provasoli P (1968) Media and prospects for cultivation of marine algae. In: Watanabe A, Hattori A (eds) *Cultures and collections of algae*. Japanese Society for Plant Physiology, Tokyo, pp 47–74
- Raven JA (1991) Physiology of inorganic carbon acquisition and implications for resource use efficiency by marine phytoplankton: relation to increased CO₂ and temperature. *Plant Cell Environ* 14:774–794
- Riebesell U, Wolf-Gladrow DA, Smetacek V (1993) Carbon dioxide limitation of marine phytoplankton growth rates. *Nature* 361:249–251
- Satoh A, Kurano N, Senger H, Miyachi S (2002) Regulation of energy balance in photosystems in response to changes in CO₂ concentrations and light intensities during growth in extremely-high-CO₂-tolerant green microalgae. *J Plant Cell Physiol* 43:440–451
- Saxe H, Ellsworth DS, Heath J (1998) Tree and forest functioning in an enriched CO₂ atmosphere. *New Phytol* 139:395–436
- Sfriso A (1995) Temporal and spatial responses of growth of *Ulva rigida* C. Ag. to environmental and tissue concentration of nutrients in the Lagoon of Venice. *Bot Mar* 38:557–573
- Somanchi A, Handley ER, Moroney JV (1998) Effect of low CO₂ growth on *psaE* and *des6* cDNAs in *Chlamydomonas reinhardtii*. In: Garab G (ed) *Photosynthesis: mechanisms and effects*, vol 5. Kluwer, Dordrecht, pp 3487–3490
- Watling JR, Press MC, Quick WP (2000) Elevated CO₂ induces biochemical and ultrastructural changes in leaves of the C-4 cereal sorghum. *Plant Physiol* 123:1143–1152
- Webber AN, Nie GY, Long SP (1994) Acclimation of photosynthetic proteins to rising atmospheric CO₂. *Photosynth Res* 39:413–425
- Wellburn AR (1994) The spectral determination of chlorophylls *a* and *b*, as well as total carotenoids, using various solvents with spectrophotometers of different resolution. *J Plant Physiol* 44:307–313
- Zimmerman RC, Hohrs DG, Steller DL, Alberte RS (1997) Impacts of CO₂ enrichment on productivity and light requirement of eelgrass. *Plant Physiol* 115:599–607